Near field and cavity effects on coupling efficiency of one-dimensional metal grating for terahertz quantum well photodetectors

R. Zhang,[1] X. G. Guo,[1] J. C. Cao,[1] and H. C. Liu[2,a)]
[1]*Key Laboratory of Terahertz Solid-State Technology, Shanghai Institute of Microsystem and Information Technology, Chinese Academy of Sciences, Shanghai 200050, China*
[2]*Key Laboratory of Artificial Structures and Quantum Control, Department of Physics, Shanghai Jiao Tong University, Shanghai 200240 China*

(Received 29 January 2011; accepted 3 March 2011; published online 11 April 2011)

The Modal Method is employed to simulate the coupling between the terahertz wave and one-dimensional (1D) transmissive metal grating on the top of terahertz quantum well photodetectors (THzQWPs). Electrical field patterns and behaviors of 1D grating at different frequencies and device thicknesses are systematically studied. The results show that, the coupling efficiency is not only determined by the grating parameters, multiple reflections in the device and the subsequent multiple diffractions at the grating also play an important role. Different diffracted modes interact with each other, and near field effect caused by the evanescent waves are essential in evaluating the coupling efficiency especially when the frequencies are below the cutoff of the gratings. The optimization conditions of the performance of 1D metal grating coupled THzQWPs are also discussed. © *2011 American Institute of Physics*. [doi:10.1063/1.3573191]

I. INTRODUCTION

Terahertz (THz, loosely defined as frequencies from 0.1 to 10 THz) science and technology have attracted more and more attention due to its potential applications in many areas, such as material identification, imaging, security screening, and communications.[1] Recently, terahertz quantum well photodetectors have been demonstrated,[2–4] which can be used in high frequency applications due to their short intrinsic lifetime of photocarriers. The intersubband transition (ISBT) selection rule requires a nonzero polarization component in quantum well (QW) direction (the epitaxial growth direction, set as z direction in this paper), which makes THzQWPs using ISBTs in the conduction band sensitive to the polarization of the radiation.[5] In the commonly used GaAs/AlGaAs system, the polarization selectivity between transverse-magnetic (TM) and transverse-electric (TE) polarization is more than 100:1.[6] But in focal plane array (FPA) applications such as real-time THz imaging system, it is necessary to use normal incident configuration where the electrical field is parallel to the QWs; therefore, some optical structures must be fabricated on the surface of the device to bend the light and cause a nonzero electrical field component perpendicular to the QWs. Gratings have been exploited by Heitmann *et al*. to excite ISBT in Si inversion layers,[7] and then they were employed in many quantum well infrared photodetector (QWIP) implementations. Different types of gratings have been extensively studied, such as lamellar gratings,[8] crossed gratings,[9] mesh gratings,[10] V grooves,[11] and random gratings[12,13] and so on. Many theoretical investigations have also been carried out to improve the coupling efficiency.[14–17] With these efforts, large-format QWIP arrays with up to 1024×1024 pixels have been demonstrated,[18] and multi-color arrays, such as four-band QWIP arrays, have also been realized.[19]

Although QWIP FPAs are commercially available, large-format array detectors in the THz range are still lacking. Recently, Patrashin *et al*. reported a grating coupled THzQWP with a 13-mA/W peak responsivity at an electric bias of 40 mV and an operating temperature of 3 K, where 1D gold grating was used.[20] The enhancement of optical effects by metallic diffraction coating in terahertz frequency has been reported in Ref. 21, and its use in THzQWP has also been theoretically studied.[22] In this paper, the effect of 1D metal grating is systematically studied with the modal method proposed by Todorov *et al*.,[23] and the coupling efficiency is investigated for different grating periods. The electrical field spatial distribution is shown to give an intuitive view of the behavior of the gratings. Our simulations predict that, first, the grating cut-off wavelength is not really the "cutoff" due to the near field effect, but the most efficient frequency point of the grating, the evanescent diffraction modes should be taken into consideration in the design of gratings; second, because the device forms a Fabry-Perot (FP) cavity in z direction, the device thickness plays an important role in coupling efficiency due to the FP cavity effect of propagating diffracted modes, and the multi-reflection in the cavity also leads to multi-diffraction at the grating. These findings are helpful to optimize grating coupled THzQWPs and construct THzQWP FPAs.

II. THEORETICAL MODEL

The modal method is used here to simulate the coupling effect of the 1D metal grating on top of THzQWPs. This method can treat a general diffraction problem of a rectangular slit metallic grating on top of an arbitrary multilayered system, which is detailed in Ref. 23; therefore, it is suitable for the problem studied here. The configuration of 1D grating

a)Electronic mail: h.c.liu@sjtu.edu.cn.

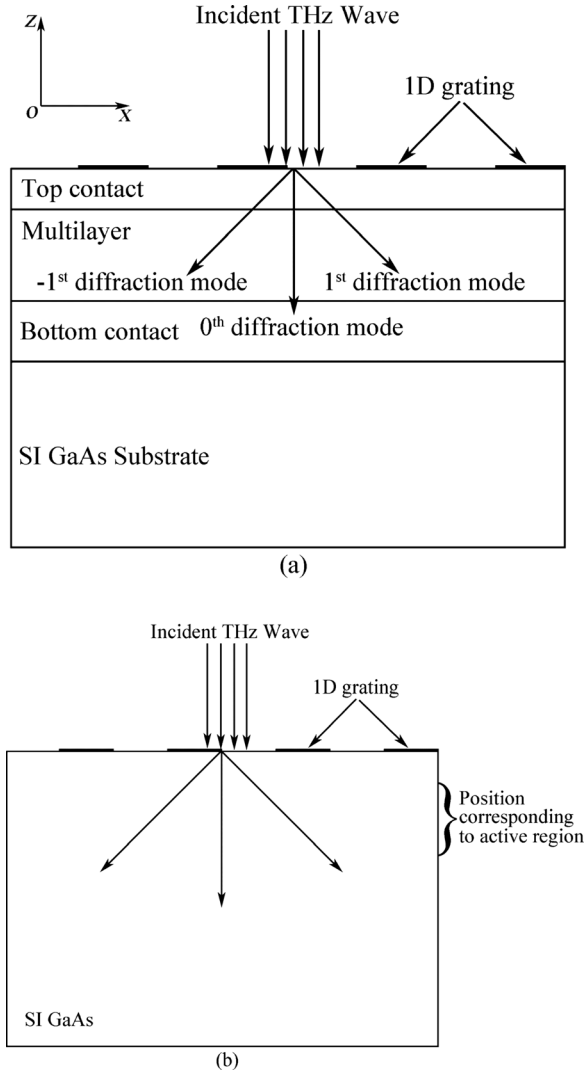

FIG. 1. (a) Schematic of 1D grating coupled THzQWP; (b) Simplified system where the region below the grating is uniform GaAs.

coupled THzQWP is shown in Fig. 1(a). For the most common THzQWP, the top and bottom electrical contacts are n-GaAs, the active region (multilayer) sandwiched between the contacts consists of tens of periods of AlGaAs barriers and doped GaAs quantum wells. Normally, the total thickness of this system is 3 to 4 μm, and the GaAs substrate below it is 600 μm. As in Ref. 22, we do not take into account the detailed structure because of the low doping density and Al fraction, and only a uniform GaAs layer shown in Fig. 1(b) is considered for simplicity. It should be noted that the substrate thickness mentioned below is the thickness of the actual substrate which is the "SI GaAs Substrate" in Fig. 1(a), and not the total thickness of "SI GaAs" in Fig. 1(b).

In this paper, the dielectric function is taken as follows: according to the Drude model for free carriers and the multi-oscillator model for optical phonons, the dielectric function of GaAs can be written as[24]

$$\varepsilon(\omega) = \frac{\omega_{\mathrm{TO}}^2(\varepsilon_{\mathrm{s}} - \varepsilon_\infty)}{\omega_{\mathrm{TO}}^2 - \omega^2 - i\omega\delta_{\mathrm{TO}}} + \varepsilon_\infty\left[1 - \frac{\omega_{\mathrm{P}}^2}{\omega(\omega + i\delta_{\mathrm{P}})}\right], \quad (1)$$

for GaAs, $\varepsilon_{\mathrm{s}} = 12.85$, $\varepsilon_\infty = 10.88$, $\omega_{\mathrm{TO}} = 2\pi \times 8.02$ THz, $\delta_{\mathrm{TO}} = 2\pi \times 0.06$ THz. δ_{P} is the damping rate depending on the doping density N_{P}, and the Drude frequency $\omega_{\mathrm{P}} = 0$ for SI GaAs.

For dielectric function of metal, the Drude model is used:

$$\varepsilon_{\mathrm{M}}(\omega) = 1 - \frac{\omega_{\mathrm{M}}^2}{\omega(\omega + i\delta_{\mathrm{M}})}, \quad (2)$$

in the case of gold, we have $\omega_{\mathrm{M}} = 1.11 \times 10^4$ THz and $\delta_{\mathrm{M}} = 83.3\ \mathrm{ps}^{-1}$.

The prototype of THzQWP studied here is V266 taken from Ref. 3, which is a typical THzQWP with response peak at 5.41 THz. The structural parameters of the active region of V266 are listed in Table I. For the simulation below, we assume that, the THz waves are normally incident from the top side of the gratings, only p-polarized light is considered, see Fig. 1; the device is large enough to omit the influence of small mesa area as observed in Ref. 25; and the intersubband absorption only weakly perturbs the pattern of electromagnetic field. Because the absorption coefficient of the electromagnetic waves is proportional to the intensity of z component of electric field, the average intensity of E_z component, set as I_{average}, in the region corresponding to the active region of V266 is calculated to characterize the coupling efficiency:

$$I_{\mathrm{average}} \propto \frac{\int_{V_{\mathrm{AR}}} |E_z|^2 dV}{V_{\mathrm{AR}}}, \quad (3)$$

where V_{AR} is the volume of active region, i.e., the volume of the "multilayer" in Fig. 1(a) or the region marked by "position corresponding to active region" in Fig. 1(b). It is worth noting that, although the device studied here is V266, the results and discussions below are applicable to common structures of THzQWPs, since I_{average} is an average quantity over the active region.

III. NUMERICAL RESULTS AND DISCUSSION

A. Influence of grating period

The grating geometry parameters are set as follows: period d, metal stripe width a, and metal stripe thickness h. The filling factor r is defined as $r = a/d$. Suppose $h = 0.38$ μm, $r = 50\%$, and the frequency of incident THz wave is the detector's peak response frequency, which is $f_0 = 5.41$ THz, the relation between I_{average} and d is simulated and given in Fig. 2.

TABLE I. The structure of V266.

	L_w (Å)	L_b (Å)	Repeat N	[Al]	N_d (cm^{-3})
V266	155	702	30	3%	6×10^{16}

L_w is the width of GaAs quantum well, L_b is the width of AlGaAs barrier, repeat N is the period number of $L_w + L_b$, [Al] is the Al fraction of the barrier, N_d is doping density in the center 100 Å of the quantum well.

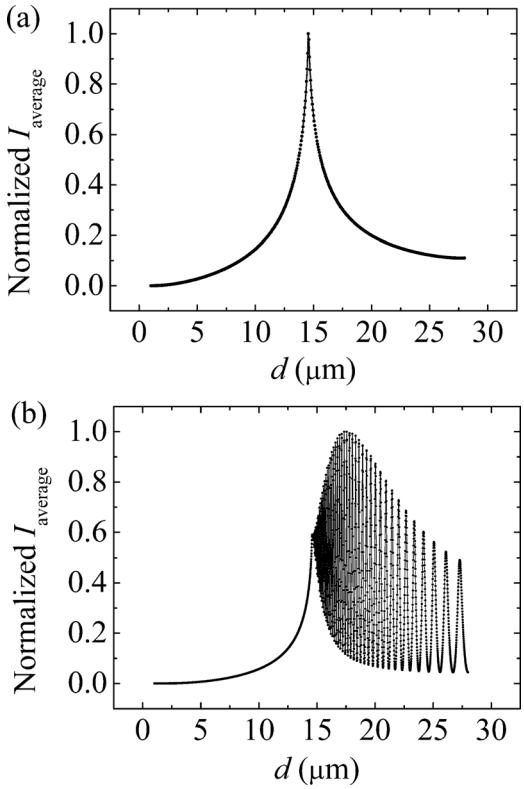

FIG. 2. The dependence of normalized $I_{average}$ (by the peak value of the curve) on the grating period d with substrate of (a) infinite thickness, and (b) 450 μm thickness. The frequency of incident THz wave is 5.41 THz.

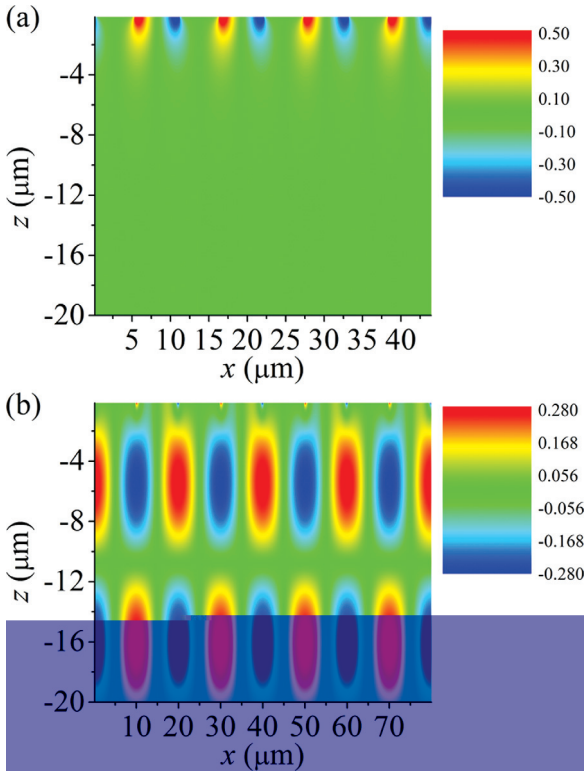

FIG. 3. (Color online) E_z pattern in the device with infinite thickness substrate. The grating is at $z = 0$ μm, and the device is below the grating. Four periods (x direction) are shown [consistent with Fig. 1(b)]. (a) $d = 11$ μm, E_z appears just below the grating, which is contributed by evanescent diffraction modes; (b) $d = 20$ μm, the pattern resembles that for multi-slit interference, and E_z distributes in the whole device because the first order diffracted mode is a propagating mode in this case.

In Fig. 2(a), the substrate thickness is infinite, the peak $I_{average}$ occurs at $d_0 = 14.6$ μm which equals to the wavelength λ of incident THz wave in GaAs, namely $d_0 = \lambda = \lambda_0/n$, in which λ_0 is the wavelength in vacuum and n is the refractive index of GaAs. On both sides of d_0, the curve is smooth. But in Fig. 2(b), oscillation appears when $d > d_0$, and d_0 is not the peak any more. In fact, the oscillation shows the FP resonance of the first order diffracted mode in the device. When $d < d_0$, f_0 is below the cutoff frequencies of the gratings, $I_{average}$ is all contributed by evanescent diffraction modes because the only propagation mode—the zeroth order diffracted mode—has no E_z component, see Fig. 3(a). Hence, the gratings with different periods behave similarly whenever the substrate is in finite. But in the condition of $d > d_0$ where f_0 is above the cutoff frequencies of the gratings, the first order diffracted mode becomes propagation wave with $k_z = \sqrt{\varepsilon k_0^2 - (2\pi/d)^2}$ [see Fig. 3(b)], in which k_0 is the wave vector in vacuum, ε is the permittivity of GaAs, and k_z is the z component of wave vector in GaAs substrate. k_z varies with d, which gives rise to intensity oscillation shown in Fig. 2(b) because of multi-reflection in the device with finite thickness (the length of FP cavity), while in the situation of infinite substrate thickness, no oscillation appears because no reflection takes place. The shift of peak intensity shown in Fig. 2(b) is due to the multi-diffraction by the gratings. It can be seen that, the substrate plays an important role in the coupling efficiency, and this influence will be discussed in more detail in the next section.

It is worth noting that, in the situation of infinite thickness substrate, the coupling efficiency reaches the maximum when the grating period $d = d_0 = \lambda$, see Fig. 2(a). However, d_0 is the so called cutoff wavelength of the grating, because for the wavelengths longer than d_0, all the diffracted modes are evanescent waves except the zeroth order which will not help due to lack of E_z component. But the fact is, since the active region is very close to the grating and the wavelength of THz wave is relative long (for the case of V266, the active region is from -0.4 to -3.0 μm in Fig. 3 and $\lambda = 14.6$ μm), the evanescent diffraction modes still can reach the active region and contribute to the ISBT, and moreover the most efficient case occurs when the frequency matches the cutoff of the grating, which also can be seen clearly in the next section.

B. Influence of substrate thickness

The purpose of this section is to investigate the influence caused by finite substrate thickness. In this case, the device will form a FP cavity in z direction. Different diffracted modes interact with each other due to multi-reflections in the FP cavity and at the grating, which will affect the coupling efficiency substantially. We set the grating period $d = 14.6$ μm which corresponds to cut-off frequency of 5.41 THz, h and r are the same as above. The relations between $I_{average}$ and frequency for substrates of infinite and finite thicknesses are shown in Fig. 4.

The case for infinite thickness substrate is shown in Fig. 4(a). The intensity peak is at 5.41 THz, which indicates that

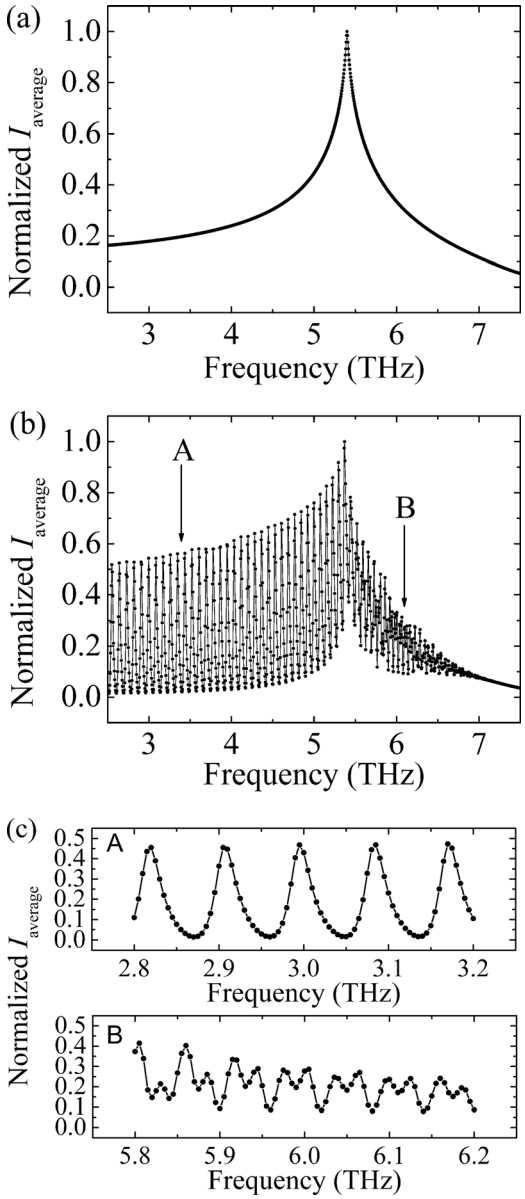

FIG. 4. The dependence of $I_{average}$ (normalized by the peak value of the curve) on frequency. (a) substrate of infinite thickness; (b) substrate of 450 μm thickness; (c) zoom in around A and B in Fig. 4(b).

the coupling efficiency is maximized when the frequency is comparable to the cutoff of the grating, and this is in agreement with the result in Sec. III A. In Fig. 4(b), the substrate thickness is 450 μm. The oscillation due to FP cavity effect can be seen clearly. There are two types of oscillations: one is at lower frequency side of 5.41 THz, which is a simple oscillation with almost uniform period of around 0.9 THz, marked as A and zoomed in shown in upper part of Fig. 4(c); the other is at higher frequency side of 5.41 THz, which is a bit irregular, marked as B and zoomed in shown in lower part of Fig. 4(c). The cutoff of the grating is 5.41 THz, hence, when the frequency is below 5.41 THz, only the zeroth order diffracted mode can propagate in the device and be affected by the FP cavity. The zeroth mode will not contribute to the ISBT by itself. However, when it is reflected back from the bottom of the substrate and meets the grating, it will be diffracted again and converted to higher diffracted modes partly, which will finally give rise to the oscillation of type A. The oscillation is consistent with the FP condition of the zeroth mode. While for the range above 5.41 THz, the first order diffracted mode also becomes a propagation mode, so both the zeroth mode and first mode will be affected by the FP cavity. But the wave vectors in z direction of two modes (set as $k_z^{0^{th}}$ and $k_z^{1^{st}}$) are different, which means different FP conditions, and moreover $k_z^{1^{st}}$ varies with the frequency, as a result two oscillations mix, resulting in the type B behavior.

These two types of oscillation can be easily understood through the dependences of $I_{average}$ on substrate thickness at the frequencies below and above the cutoff, which are given in Fig. 5 for the same grating parameters as in the above. In Fig. 5(a), the frequency of incident light is 4.5 THz, which is below the cutoff. The corresponding wavelength λ in GaAs is 17.98 μm, which is also the wavelength of the zeroth order

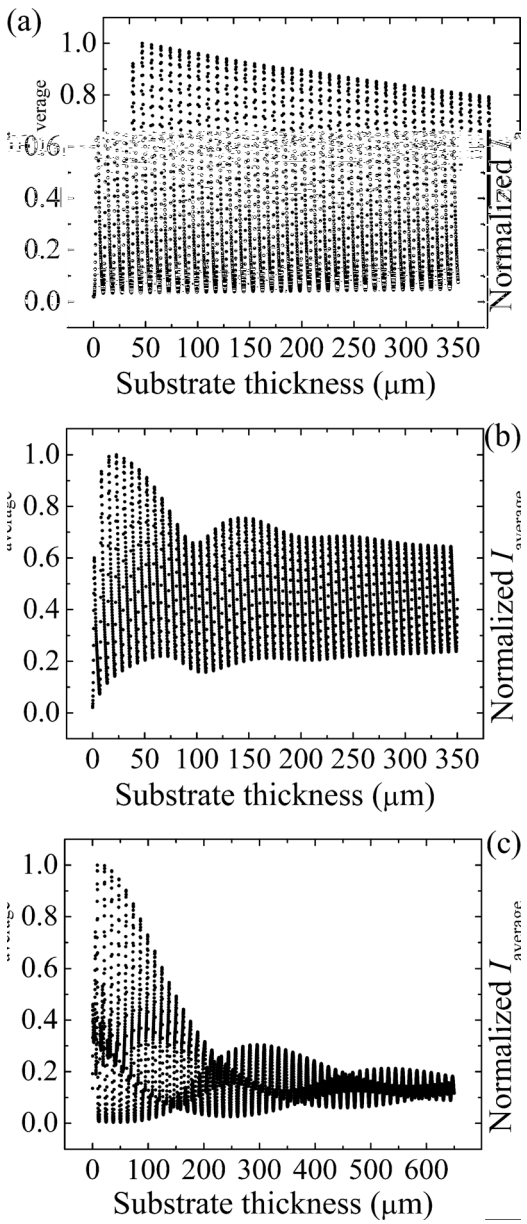

FIG. 5. Calculated $I_{average}$ (normalized by the peak value of the curve) versus substrate thickness. (a) $f = 4.5$ THz; (b) $f = 5.41$ THz; and (c) $f = 6.0$ THz.

diffracted mode in z direction. The calculated period of the oscillation shown in Fig. 5(a) is around 9.0 μm. This implies that, from one oscillation peak to the next, the difference of the round-trip path within the cavity is just the wavelength of the zeroth mode. So the oscillation is caused by the interference of the zeroth mode in the FP cavity. The zeroth mode is enhanced by the constructive interference, then it is converted to higher order evanescent diffraction modes by the multi-diffraction at the grating, which results in a peak in the oscillation of I_{average}. Similarly, the destructive interference makes a valley in the oscillation. The reduction of the oscillation amplitude as the increase of the thickness is due to the small imaginary part of refractive index of SI GaAs, which leads to the absorption. For the incident light of 5.41 THz shown in Fig. 5(b), which is almost the cut-off frequency of the grating, it is similar with the situation of 4.5 THz. Because the first order diffracted mode travels nearly parallel with the QWs, i.e., $k_z^{1^{\text{st}}} \ll k_z^{0^{\text{th}}}$, the oscillation is mainly formed by the zeroth mode, where the wavelength is 14.6 μm and the period of the oscillation is 7.3 μm. When the frequency is above the cutoff, the oscillation becomes more complicated. For example, for incident light of 6.0 THz, the wavelength of the zeroth order diffracted mode in z direction is 12.76 μm, while it is 26.68 μm for the first order diffracted mode. The two modes interfere with each other resulting in different constructive and destructive conditions, and then induce a composite oscillation behavior shown in Fig. 5(c). We can expect more complex oscillation when the second or even higher order diffracted modes become propagation modes.

IV. CONCLUSION

We have studied the coupling effect of 1D metal grating for THzQWPs. The results show that, the cut-off frequency is not really cutoff, and the grating still works below it due to the evanescent waves. The consequence of multi-reflection and multi-diffraction due to finite substrate thickness has been discussed. The FP cavity makes the coupling efficiency oscillate with the substrate thickness when the propagation diffracted modes travel in the cavity, and the type of the oscillation depends on the number of propagation modes. So for the optimum detection of a grating coupled device, not only the grating parameters should be considered, a proper substrate thickness is also important, especially in the detection of a monochromatic light, for example, from a THz quantum cascade laser. It should be mentioned that, although the gratings discussed here are for THzQWPs, the results are also applicable to detectors in infrared range.

ACKNOWLEDGMENTS

This work was supported in part by the National Basic Research Program of China (Grant No. 2007CB310402), the 863 Program of China, the National Natural Science Foundation of China (Grant No. 60721004), the major projects (Project Nos. KGCX1-YW-24 and KGCX2-YW-231), the Hundred Talent Program of the Chinese Academy of Sciences, and the Shanghai Municipal Commission of Science and Technology (Project Nos. 10JC1417000 and 11ZR1444200).

[1] B. Ferguson and X. C. Zhang, Nature Mater. **1**, 26 (2002).
[2] H. C. Liu, C. Y. Song, A. J. SpringThorpe, and J. C. Cao, Appl. Phys. Lett. **84**, 4068 (2004)
[3] H. Luo, H. C. Liu, C. Y. Song, and Z. R. Wasilewski, Appl. Phys. Lett. **86**, 231103 (2005).
[4] M. Graf, G. Scalari, D. Hofstetter, J. Faist, H. Beere, E. Linfield, D. Ritchie, and G. Davies, Appl. Phys. Lett. **84**, 475 (2004).
[5] H. Schneider and H. C. Liu, *Quantum Well Infrared Photodetectors: Physics and Applications* (Springer, Berlin, 2006).
[6] H. C. Liu, M. Buchanan, and Z. R. Wasilewski, Appl. Phys. Lett. **72**, 1682 (1998).
[7] D. Heitmann, J. P. Kotthaus, and E. G. Mohr, Solid State Commun. **44**, 715 (1982).
[8] K. W. Goossen and S. A. Lyon, Appl. Phys. Lett. **47**, 1257 (1985).
[9] J. Y. Andersson and L. Lundqvist, Appl. Phys. Lett. **59**, 857 (1991).
[10] Y. C. Wang and S. S. Li, J. Appl. Phys. **75**, 8168 (1994).
[11] C. J. Chen, K. K. Choi, M. Z. Tidrow, and D. C. Tsui, Appl. Phys. Lett. **68**, 1446 (1996).
[12] G. Sarusi, B. F. Levine, S. J. Pearton, K. M. S. Bandara, and R. E. Leibenguth, Appl. Phys. Lett. **64**, 960 (1994).
[13] S. I. Borenstain, U. Arad, I. Lyubina, A. Segal, and Y. Warschawer, Appl. Phys. Lett. **75**, 2659 (1999).
[14] J. Y. Andersson and L. Lundqvist, J. Appl. Phys. **71**, 3600 (1992).
[15] G. Sarusi, B. F. Levine, S. J. Pearton, K. M. S. Bandara, R. E. Leibenguth, and J. Y. Andersson, J. Appl. Phys. **76**, 4989 (1994).
[16] E. Dupont, J. Appl. Phys. **88**, 2687 (2000).
[17] Y. Fu, M. Willander, W. Lu and W. Xu, J. Appl. Phys. **84**, 5750 (1998).
[18] S. D. Gunapala, S. V. Bandara, J. K. Liu, C. J. Hill, S. B. Rafol, J. M. Mumolo, J. T. Trinh, M. Z. Tidrow, and P. D. Levan, Proc. SPIE. **5783**, 789 (2005).
[19] S. V. Bandara, S. D. Gunapala, J. K. Liu, S. B. Rafol, D. Z. Ting, J. M. Mumolo, R. W. Chuang, T. Q. Trinh, J. H. Liu, K. K. Choi, M. Jhabvala, J. M. Fastenau, and W. K. Liu, Infrared Phys. Techn. **44**, 369 (2003).
[20] M. Patrashin and I. Hosako, Opt. Lett. **33**, 168 (2008).
[21] A. K. Azad and W. Zhang, Opt. Lett. **30**, 2945 (2005).
[22] P. Hewageegana and V. Apalkov, Infrared Phys. Techn. **51**, 550 (2008).
[23] Y. Todorov and C. Minot, J. Opt. Soc. Am. A. **24**, 3100 (2007).
[24] J. S. Blakemore, J. Appl. Phys. **53**, R123 (1982).
[25] A. D. Rossi, E. Costard, N. Guerineau, and S. Rommeluere, Infrared Phys. Techn. **44**, 325 (2003).